Performance Enhancement of Solar Air Heater by Integrating Innovative Absorber Design and Automatic Control Flow Rate

Louay A. Rasheed
Department of Electromechanical Engineering, University of Technology, Iraq

Jamal A.-K. Mohammed
Department of Electromechanical Engineering, University of Technology, Iraq

Raed A. Jessam
Department of Electromechanical Engineering, University of Technology, Iraq

https://doi.org/10.5109/7151693

出版情報：Evergreen. 10 (3), pp.1439-1448, 2023-09. 九州大学グリーンテクノロジー研究教育センター
バージョン：

Performance Enhancement of Solar Air Heater by Integrating Innovative Absorber Design and Automatic Control Flow Rate

Louay A. Rasheed[1], Jamal A.-K. Mohammed[1], Raed A. Jessam[1,*]
[1]Department of Electromechanical Engineering, University of Technology, Baghdad, Iraq

E-mail: 50097@uotechnology.edu.iq

(Received July 17, 2023; Revised August 31, 2023; accepted September 2, 2023).

Abstract: Solar air heater is often used to warm air for residential heating and drying agricultural products. Developing a single-pass absorber of the solar air heater in the form of a wire mesh layer will significantly improve its performance under certain climatic conditions. To further increase the efficiency of the modified solar heater so that it can adapt to all climatic conditions, an automatic control system combined with a fan motor has been designed and integrated with the heater to provide it with suitable parameters such as temperature and airflow rate. To determine the effect of the automatic fan speed control affects solar air heater performance, an experimental investigation is presented in this paper. Under identical weather conditions, two tests were conducted for two consecutive days, one without and one with using automated fan speed control. The control system was programmed to regulate outlet air temperature with a range of 40-60 °C. Accordingly, the fan speed is automatically changed in response to temperature variations. Online monitoring and adjustment of temperature will increase air temperature stability and stop oscillations despite varying solar radiation levels during daytime hours. With greater thermal efficiency than conventional technique, this technology encourages more even airflow and improved heat transfer, raising surface temperatures in the heater duct. By using automated control, the thermal efficiency of the heater is increased by roughly 39.5 %.

Keywords: automatic control system; fan speed; solar air heater; thermal efficiency; wire mesh absorber layer.

1. Introduction

Air or water can be employed as the principal heat transfer fluid in solar heating and cooling systems. The simplest use of solar thermal energy is the solar water heater (SWH)[1,2]. On the other hand, the SAH is solar thermal equipment that uses insolation to heat air by absorbing it. The SAH uses renewable energy for heating or cooling the air in buildings or for industrial processes. In low-temperature operations the SAHs are a common form of heat exchanger. A variety of industries can make use of the heat produced by the SAHs to dry agricultural products[3-5] and as backup heaters in homes and residential applications[6,7], for instance and to conserve power during the hot months. A domestic solar heating unit with high level of automation, specially designed to reduce energy consumption in Brazil[6]. The investigated system proved to be economically viable, saving expressive quantities of electrical energy and water if compared to traditional systems. The absorber plate is an essential part of SAH that converts solar energy into heat. A low heat transfer coefficient occurs between the absorbent plate and the moving air as a result of the thermophysical feature of air. This is causing the SAHs' primary flow to become apparent. To significantly improve the SAH's energy efficiency, extended, corrugated, and finned surfaces, baffles, barriers, and baffled surfaces on the absorber surface can all be adopted. Numerous attempts to increase SAH effectiveness have been undertaken in earlier studies relating to this topic. The best-performing barrier was one with a pentagonal shape, demonstrating how the structure and design of the barrier affect the SAH's effectiveness. Karsli[3] evaluated the first and second rules of efficiency for four different kinds of flat plate SAHs. The experiment's findings revealed that the design of the heater and sun radiation has a significant influence on how well the SAH performs. Experimental research was done to estimate the energy efficiency of three different kinds of double-flow SAHs that used aluminum cans. The barriers or cans, according to an experimental investigation by Ozgen et al.[8], ensure proper airflow to the absorption plate, create turbulence, and reduce heater dead zones. To determine the energy and exergy content of five distinct kinds of solar air absorbers, Benli[9] carried out an experimental analysis. The results show that the surface shape of the absorber affects both the pressure drop and the heat transfer coefficient. Reducing the geometrical characteristics of various roughness, the

higher-pressure drop may be increased. The ribs or energy promoters which fixed on the surfaces has a wide application to increase pressure coefficient of air flow by reducing its velocity[10-12]. Kulkarni and Kim[13] quantitatively studied four different barrier shapes and three unique combinations in SAHs. Through the use of numerous solar air collectors, Jalil et al.[14] evaluated the performance in high air temperature conditions. The results showed that it is easy to figure out how many collectors need to be linked in series to get the appropriate output air temperature. Singh et al.[15] performed an experimental investigation on the effects of using double-pass converging inclined fins and wire mesh on the effectiveness of SAH. Double-pass SAHs with wavy fin absorbers were the subject of an experiment carried out by Jalil et al.[16]. The absorber's lower and upper surfaces were joined to the fins. When wavy absorber findings are compared to those of flat absorbers, the thermal efficiency improvement was 80% and 84% for 3 and 7 wavy absorbers, respectively. To establish the greenhouse impact and capture solar energy, Ismaeel et al.[17] built a SAH as part of an atmospheric electric power generation model on a top layer that was twice as transparent. This allowed hot air to travel to the component that produces electricity. The results of the study demonstrated that increasing the number and surface area of the collector's skin SAHs enhances system performance. Providing a coating on the surface of the absorber can improve the performance of a triangle SAH. On absorber surfaces, Kumar et al.[18] conducted a comparison of commercial paint coatings made using graphene-black paint and graphene/CeO2-black. In both instances, black paint with 2% nanomaterial incorporated in it is employed as a coating agent. Hussein et al.[19] investigated the effect of pulsing flow as an active technique on the thermal efficiency of a double-pass SAH using a tubular solar absorber. Based on the results of the experiment, it was concluded that applying pulsing flow increases the rate of heat transfer. It was discovered that applying pulsating flow causes the outlet temperature to increase by roughly 25.6–27% when compared to the constant flow condition.

To increase the efficiency of the SAHs, the absorption plate of the SAH was reconfigured by Rasheed et al.[20] in the form of a wire mesh layer and tilted at a specific angle. For three different mass flow rates, the heater was studied and contrasted with a conventional flat absorber plate. The modified SAH was shown to have significantly greater thermal efficiency than the conventional one. It promotes more even airflow through the absorber, increases the surface area, and accelerates heat transfer, all of which lead to higher surface temperatures in the duct.

One of the critical tasks in many automated systems is that adopts a feedback approach to the temperature of any room due to solar radiation to achieve automatic heat regulation. These systems need to use specialized sensors, from basic to sophisticated ones, and environmental monitoring software, to enable measuring and viewing the temperature value in the space. The regulation of room temperature is a topic that is extensively covered in research papers in the literature. The most significant may be summed up as follows:

The temperature inside a room may be adjusted by using a fan speed control system. V. Bhatia and G. Bhatia[21] developed a fan PWM speed control system depending on temperature variations inside the room. Kesarwani et al.[22] created a case study to regulate the temperature in systems utilizing microcontrollers, TRIACs, and bridge rectifiers. The design and development of a temperature distribution control system used in a neonatal incubator were proposed by Widhiada et al.[23] to guarantee a baby's utmost wellness. A microcontroller-based incubator system was used in the experiment for temperature detection, control and humidity management. This has shown to be a very helpful tool for infant care and well-being. A temperature control system concept that might be executed on the Tudung Saji microcontroller was proposed by Abdullah et al.[24] utilizing Arduino IDE. Simulation software and experiments were applied to find the results. This research aims to prevent bacteria when a certain temperature has been attained. Because bacteria can be eliminated at a specific temperature, the software looks to be highly effective at controlling and even preventing bacteria. Through manual measurements using analog instruments like thermometers, hygrometers, and manometers, earlier measurements on Server Room Temperature (SAR) had been made to efficiently estimate air temperatures. The monitoring and control of these parameters are greatly hampered by simple manual measurements. Yu et al. 2011[25] developed a control system that uses a wireless sensor network for ideal temperature management, making it simpler for operating and monitoring the conditions at any time. This effectively solved this problem. Logging is the procedure of gathering, analyzing, and storing data and events when performing a testing procedure using a system or a product. Sensor control is a component of data logging, which is used to collect and analyze data for monitoring systems and scientific research[26-27]. Any type of transducer's electrical output may be automatically measured, and the value can be logged because the user specifies the type of information to be recorded, such as light intensity, temperature, relative humidity, voltage, etc.[28-29]. It is possible to utilize a standard personal computer-based data-gathering system, but this option is, firstly, more expensive because it requires both a computer and a data logger. Secondly, the size is substantial. Thirdly, a strong battery pack is needed in a situation where there is no main supply because the power assumption is going to be high[30]. Pradhapraj and Sivarathinamoorthy[31] used the LabVIEW interface, which combines several sensors into a single system, for real-time monitoring of the performance of SAHs. Data acquisition (DAQ) made it possible to collect data such as temperature, humidity, sun

intensity, and user utilization of data queries. Jumaat and Othman[32] measured solar panel properties using a variety of sensors, including a temperature sensor to gauge the panel's temperature, an LDR sensor to gauge light intensity, a voltage divider to gauge output panel voltage, and a current sensor to gauge the panel's output current. The outputs from these sensors were utilized by Arduino to demonstrate data on the Liquid Crystal Display (LCD). To merge all components into one platform and operate consecutively, Pramod et al.[4] created an open-source-based software application. A developed data recorder was tested in a 100 kg capacity powered by sunlight, an air-inflated drier, and a grain storage structure with a capacity of 0.5 tons. In the developed SAH, moisture decreased in the range of 22-14% (w.b) and finished in 7.5–9 hr as opposed to 11–12.8 hr in the sun. Raed and Han[33] were investigated a hybrid inclined solar chimny, by integrating the inclined solar chimney with an external heat source at an average temperature of only 88.0℃. The results show that the mean enhancement in the air temperature rise of the hybrid mode is 33% compared to the solar mode

The modified SAH[20] will be modified to works more efficiently and adapt to all regions and climatic conditions. The present paper was adopted an experimental test through design an automatic control system, integrated with the heating system to provide it with appropriate parameters such as temperature and airflow. For fast heating rates, an electric fan is used to produce a hot air stream. The fan speed is automatically changed in response to temperature variations. Although there are many data acquisition systems available today, they are expensive and have a lot of functions that may not be necessary for the proposed application. Consequently, this heater uses a cost-effective, customized, real-time monitoring of air specifications by the required temperature and air velocity during the heating process. The proposed SAH has been developed with open-source hardware and software, which makes it simple for us to online control and monitor temperature as well as the amount of airflow.

2. Research methodology

The proposed SAH system is generally built in two stages, the first stage is the construction of the SAH, and the second stage is the design of the automatic control and monitoring system.

2.1 Construction of the solar air heater

Figure 1 shows the overall setup of the proposed SAH system. The proposed heater comprises several components, a heating absorber plate, glazing, wire mesh layer, rigid frame, inlet duct, outlet duct, and insulator layer. The heated absorbent plate has a metal frame and is (1500 × 900 × 1) mm in size. The solar radiation transparent penetrated surfaces (glasses) have dimensions of 1500 mm by 900 mm and a thickness of 4 mm. The bottom and sides were insulated with polyurethane foam, and the absorber's net area is (1500 × 800) mm. It is built of aluminum sheets and painted with a dark black color.

Fig. 1: The overall setup of the proposed SAH system

Between the surface of absorber plate and the surface of glass panel, there is an 80 mm air-moving gap. The SAH has a mesh layer absorber made of aluminum wire that measures (1502 × 800) mm. With the help of a wire mesh absorber layer, the SAH system works to warm the air by absorbing solar radiation. The wire mesh is located diagonally with a tilt angle of 3° over the bottom insulator and under the glass cover. At the heater's air entry, the wire mesh layer is fixed to the upper surface of the duct, and at the air exit, it is fixed to the lower surface of the duct. The air driven by an electric fan enters the heater's duct and passes through slots in the wire mesh within the opening along the SAH duct. The air inlet and outlet area in the heater duct is (60×700) mm.

The wire mesh layer comprises wires with a 0.795 mm diameter and a 2.5 mm pitch. Two SAHs were constructed, one without electrical control and the other integrated with the automatic control and monitoring system. Figure 2 illustrates the schematic assembly of the SAH with a wire mesh layer absorber. The primary characteristics of the SAH are listed in Table 1.

Table 1: Characteristics of the SAHs

Items	Characteristics
Type of flow	Single-front pass
SAH box	Steel sheet 0.80 mm thickness, 900 mm×1500 mm×150 mm
Insulator	50 mm polyurethane foam
Absorber	From Aluminum, 900×1500×1 mm
Glass	4 mm tempered glass, normally ironed, 90% transmittance
Coated absorber	0.20 - 0.49 Emissivity, 0.88-0.94 Absorptivity
Fan	Cross-flow cooling fan (12V, 4.8W)

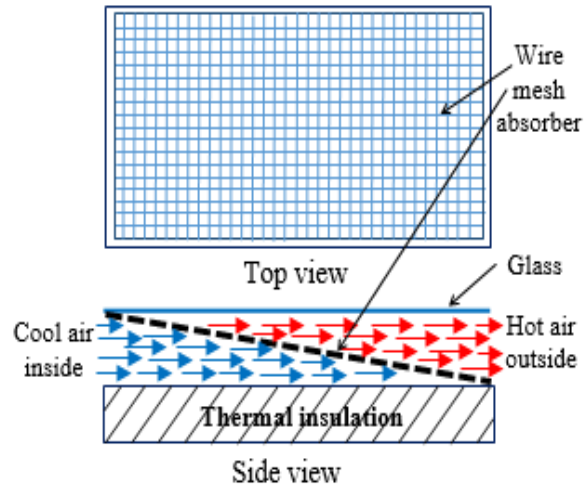

(A)

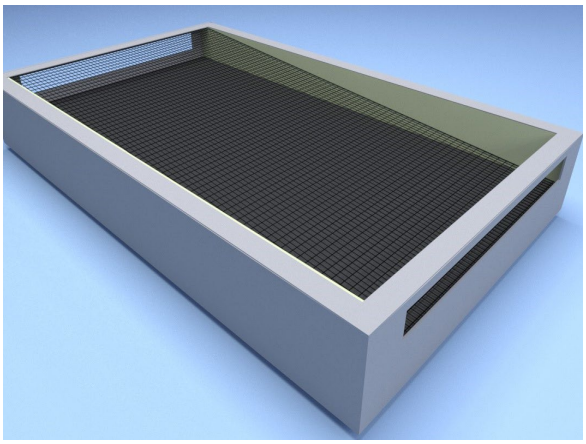

(B)

Fig. 2: Assembly of: A) schematic of SAH, B) image of the SAH with wire mesh layer absorber

2.2 Implementation of automatic control and monitoring system

The suggested heating system has three steps that it goes through to operate. A DHT11 temperature sensor is used in the first step to measure the temperature. The second step gets the temperature values from the DHT sensor module, transmits them to Arduino, and then transforms them into a meaningful percentage and a number in Celsius. Monitoring is the third step of the operation system, and it employs an LCD to provide temperature information. Single-wire serial communication is employed for data transmission between devices. The sensor module receives a start signal from the Arduino before receiving a response signal with information about the temperature. With a temperature range of 40 to 60 °C, the automated control system was set up to manage output air temperature. As a result, the fan speed adjusts itself automatically in reaction to temperature changes. As shown in the circuit schematic diagram of Fig. 3 and setup in Fig. 4, the following components make up the hardware of the control and monitoring system:

- Arduino Uno.
- DHT22 Sensor
- L293D Motor Driver IC
- 12 V DC Fan motor
- 12V Battery
- 16×2 LCD Display
- 2.2 kΩ Potentiometer
- Breadboard
- Uno

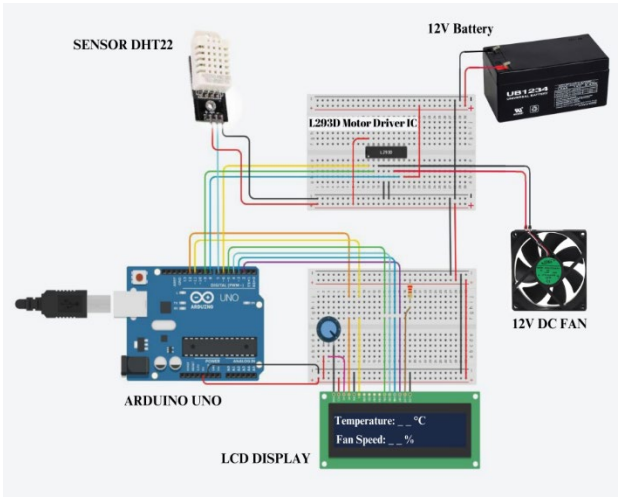

Fig. 3: Assembly circuit schematic diagram of the temperature-based fan speed control and monitoring system.

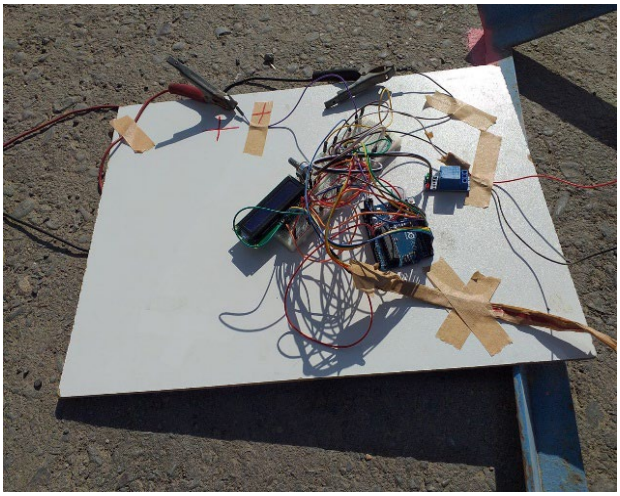

Fig. 4: Setup shows the temperature-based fan speed control and monitoring system

2.2.1 Arduino UNO board

The Arduino boards are available in a range of sizes and forms. The Arduino UNO is the most popular model, which has been used in the current study. It controls every aspect of how the SAH works. The microcontroller board called UUO uses the ATmega328P. On this board, there are six analog inputs, a 16 MHz quartz crystal, a power connector, a USB connection, an ICSP header, and a reset

button. There are also 14 digital input/output pins (with six of them being PWM outputs). Everything that is needed to get started with the microcontroller is included. It just requires the user to plug it into a USB port on a computer, use an AC-to-DC converter to power it or use a battery.

2.2.2 Temperature and humidity sensor board

A DHT22 sensor is used to measure the temperature, which is then used to control the fan speed. This sensor comes in a 4-pin single-row device and has an integrated resistive-type humidity measuring component, an NTC-type temperature measurement element, and an 8-bit microcontroller with a quick reaction time. Serial communication, also referred to as "single-wire communication", is used by the DHT22 module. When compared to other sensors, this one is incredibly user-friendly and extremely accurate. This module transmits data as a pulse train for a predetermined period. It also takes about 4 m/s for the entire process. To ensure DHT detection, the Arduino delivers a high-to-low starting signal to DHT22 at the beginning. After pulling up the data line, the Arduino waits for 20–40 sec for the DHT to react. With an 80 sec time delay after receiving the start signal, the DHT sends an Arduino with a low voltage level response signal. The SAH system uses DHT22 sensors to measure the outlet air temperature of the SAH. According to the sensor's reading, the fan speed is changed. The Arduino UNO is used to receive and analyze the data collected from the sensor. The SAH exhaust fan performs temperature regulation when it removes excess moisture but the parameters remain below the required temperature limit**.**

2.2.3 L293D DC fan motor driver

When rapid heating rates are necessary, the heated air stream can be produced by an electric fan. A cross-flow cooling DC fan motor (12 V, 3.6 W) is used and driven by L293D driver IC as shown in Fig. 3. For managing the SAH's air flow rate, this driver and Arduino are combined to send appropriate PWM signals with different duty cycles to the DC fan motor. By sending these signals, the motor speed is managed [27]. Five different settings are changed using the proposed software to control the fan. The fan will be turned off and data will be demonstrated on the LCD if the value of temperature falls below 40°C. If the temperature is between 40 and 45 ºC (25% duty cycle), the DC fan will begin operating at a low speed. The fan will operate at medium speed if the temperature is between 45 and 50 °C (50 % duty cycle). When the temperature fluctuates between 50°C and 55°C, the fan will operate at high speed (75% duty cycle). Finally, the fan will operate at its highest (full) speed if the temperature is greater than or equal to 55°C (100% duty cycle).

2.2.4 Liquid crystal display LCD

An LCD is employed to monitor the temperature data in the SAH and provides data while controlling the air conditions leaving the SAH. The LCD shown in Fig. 2, which is directly connected to Arduino in 4-bit mode, shows the temperature and airflow rate readings. The LCD's RS, EN, and D4-D7 pins are connected to the Arduino's digital pins 2–7. Additionally, a DHT11 sensor module is connected to Arduino's digital pin 12 using a 5k pull-up resistor.

3 Experimental Procedures

Several experiments must be carried out as part of the SAH's research and development procedure to test the SAH's effectiveness. Measuring will be integrated with the SAH setup to record the required readings. The total effectiveness of the SAH system depends on a variety of factors. Experimental tests were conducted on 3rd and 4th May 2023 in Baghdad city, Iraq (33.333° latitude, 44.433° longitude) from 7:00 am to 5:00 pm during sunny weather. Iraq is located in a Northern Hemisphere location that has good access to solar energy. It was assumed that the heater's slope matched the value of the local latitude. The thermal performance of the proposed SAH using a wire mesh layer on a flat plate for two operation modes was investigated and experimentally evaluated in this study. The first mode is without use of a control system on the speed of the fan motor, a constant fan speed (CFS) at a value of 0.3 m/s, while the other mode employs an automatic control system that controls the airflow rate and temperature regulation via using automatic variable fan speed (VFS). The VFS mode utilizes an automated operation with temperature-based fan speed control and monitoring based on online data coming from the DHT22 sensor under the supervision of an Arduino controller.

The primary function of the proposed absorption panel is to capture heat from the incident solar radiation. This action leads to heating the air passing through the SAH. The benefit of adding a wire mesh absorption layer is that it makes the airflow uniform, improves thermal conductivity, and raises the air temperature. The setup of the temperature control and monitoring system illustrated in Fig. 4 shows how to wire up the Arduino with all of the necessary parts for temperature-based fan motor speed monitoring and control. The DHT22 sensor is positioned in front of the SAH's air outlet to estimate the air temperature as shown in Fig. 5. Based on the amount of solar radiation and the heated air temperature, the fan speed is automatically adjusted.

Fig. 5: Measuring the air temperature via the DHT22 sensor

According to the requirements of the control system, the fan speed is programmed via four PWM signals (with different four values of duty cycles coming from the Arduino to get four different values of air flow rate. The air speeds were measured by the anemometer at the SAH outlet as shown in Table 2.

Table 2: Characteristics of the measurement instruments.

Readings	Duty cycle (%)	Air speed (m/s)	Air flow rate (kg/s)
1	25	0.14	0.0075
2	50	0.3	0.015
3	75	0.45	0.0225
4	100	0.6	0.03

The system's brain, the Arduino, manages all operations. The voltage signal that outputs from the DHT22 is proportional to the measured temperature in Celsius. The operational range for temperature is 40–60 °C. The sensor output is used to calibrate a digital signal. For the case of CFS mode, two groups of T-type thermocouples were utilized for measuring temperature data during the first stage of the operation. The first group measures the exit temperature T_o values at a point 3 cm in front of the orifice meter as shown in Fig. 6, while the second group measures the entrance temperature T_i. Data on air temperature, air velocity, and solar radiation were collected from 7 am to 5 pm.

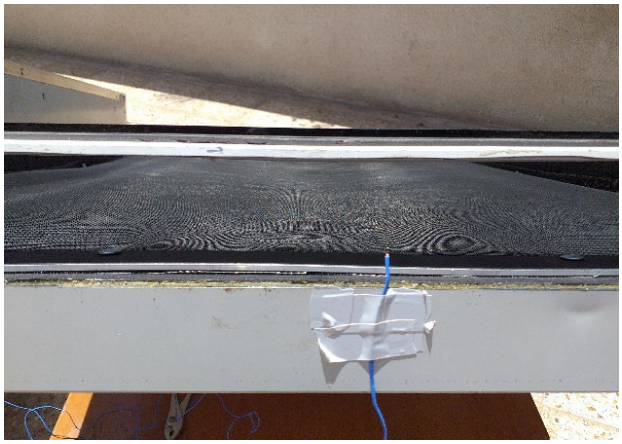

Fig. 6: Measuring the air temperature in the case of CFS

4 Thermal Analysis

Equation 1 has been used to describe the air mass flow rate. While Equation 2 and Equation 3 have been used to find the SAH's efficiency and the heat gained by the SAH depending on the mass flow rate, respectively. These equations were utilized to analyze the thermal performance of the solar air heating system:

$$\dot{m_a} = \rho\, A\, V \tag{1}$$

$$\eta_c = \frac{\dot{m_a}\, C_{pa}\, (T_o - T_i)}{A_c\, I} \tag{2}$$

$$Q_u = \dot{m_a}\, Cp_a (T_o - T_i) \tag{3}$$

5. Results and Discussion

Figures 7 and 8 depict the exterior climatic conditions for the two successive days, the third and fourth of May 2023, corresponding to the two modes of operation, CFS and automatic VFS. These two days were found to have almost the same solar strength. The highest worldwide solar radiation in the SAHs' was measured with a value of 965 W/m^2 at 12:00 in the CFS mode, while it was measured by 940 W/m^2 in the automatic VFS mode at 12:00 in the VFS mode. Radiation is low in the morning, steadily building up to a peak around midday, and then gradually decreasing until it reaches its lowest point around sunset. The ambient temperature followed a similar pattern to solar radiation and peaked at 15 o'clock.

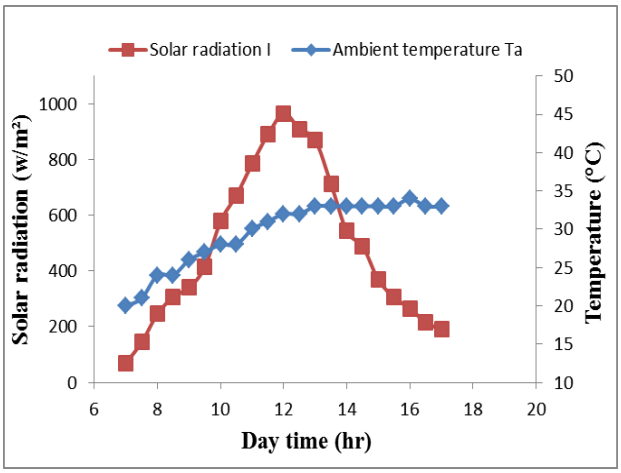

Fig. 7: Variation solar radiation and ambient temperature vs. standard local time for the CFS mode (3 May 2023).

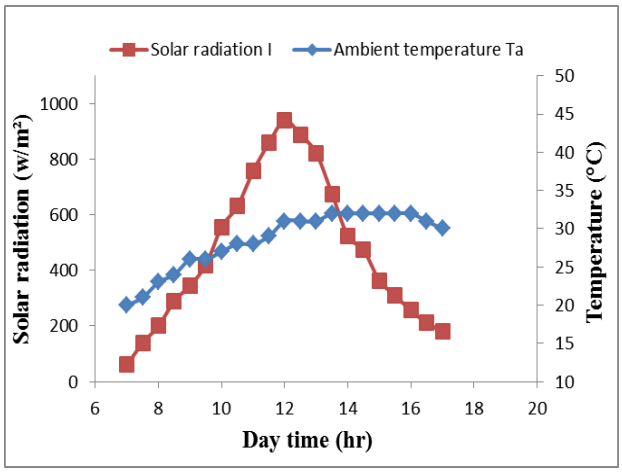

Fig. 8: Variation Solar radiation and ambient temperature vs. standard local time for the VFS mode (4 May 2023).

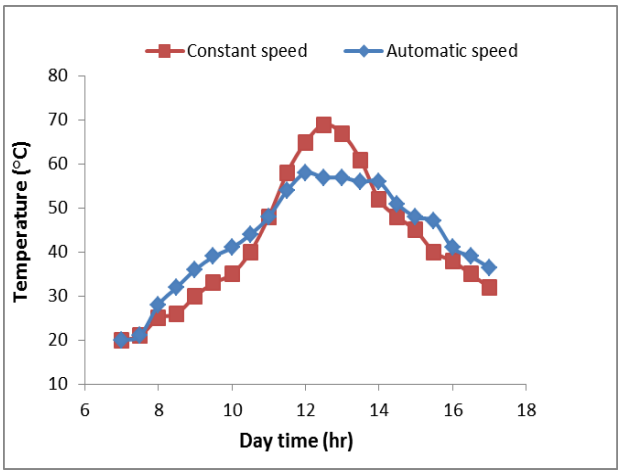

Fig. 9: Temperature of the outlet of SAH with the local time under the two operation modes.

Figure 9 shows the change of temperatures of the outlet air (T_{o1}, T_{o2}) of the SAH in the two modes of operation control, the CFS and automatic VFS, respectively. The daily average outlet air temperature in the AFS case is considered higher compared to that of the CFS case, specifically, during the peak hours in the middle of the day. The temperature VFS curve relatively drops due to the automatic increase in the fan speed as a result of the activation of the control system.

For the fan speed control mode (VFS curve), it is observed that the temperature increases somewhat more than the constant fan speed mode (CFS curve) during the daylight hour periods in the morning (8-10:30) hr as well as after midday in the period (14-17) hr, as solar radiation is weak. This is because the automatically controlled fan in the VFS mode runs at a low speed associated with the low temperature at that time as compared to the constant fan speed in the case of CFS mode. The difference is clear because the air is almost static and does not flow over the static surface and depends only on the force of the buoyancy. But it is noticed, in the middle of the day during the period (11-14) hours, that the CFS curve rises above the automatic VFS curve, as the fan speed increases automatically due to elevate temperature rates during this period until it reaches its peak value at 12:30, and thus the flow rate increases, while the flow rate remains constant in the CFS mode, despite the temperature rises in this mode to higher levels than the VFS mode.

Figure 10 shows the variation in thermal efficiency of the SAH during the day under the two operation modes. It is noted that maximum efficiency values appear in the middle of the day as a result of the high rates between the inlet and outlet temperature difference and solar radiation.

According to the results of the experiments, the average thermal efficiency of the SAH with the wire mesh layer under constant fan speed (CFS) was 31.9%, whereas it was 44.5% for the heater when it was combined with an automated fan speed control system (VFS). This indicates that the heating system's efficiency has increased by 39.5%.

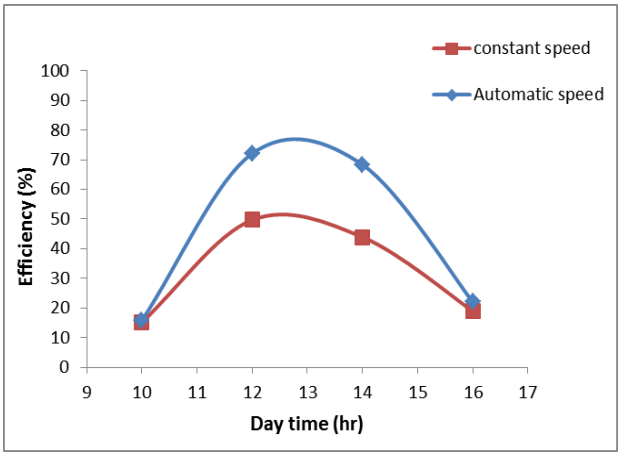

Fig. 10: Variation of thermal efficiency vs. local time for the SAH under the two operation modes.

Figure 11 shows the sun's irradiance and the corresponding automatic variations in fan speed throughout the day. From sunrise until midday, both radiation and fan speed gradually rise according to changing SAH temperatures until they peak at (12-15) o'clock and then both fall until sunset, resulting in efficient automatic fan speed adjustments in response to temperature and solar radiation levels.

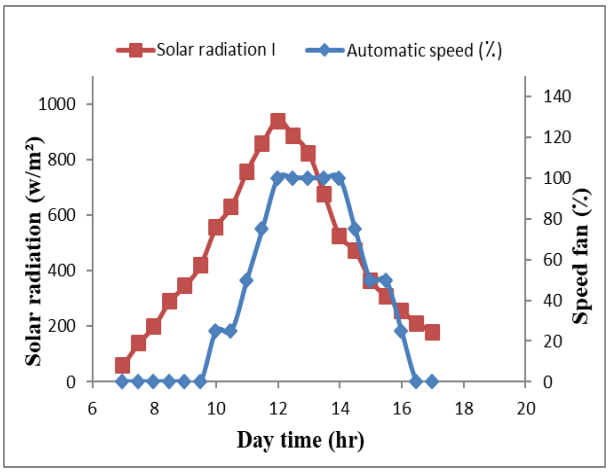

Fig. 11: Variation of solar radiation and fan speed with time in the automatic VFS mode.

6. Conclusions

This study presents the design and implementation of automatic control and its effect on the performance of a SAH equipped by a wire mesh absorber at different speed of air (0.14 m/s, 0.3 m/s, 0.45 m/s and 0.5 m/s). From the collected data and the calculated results, it can be deriving the following conclusions:

- The results show the usability of the system has been enhanced by several advanced features, such as providing the necessary temperatures and hot air streams for thermal applications in various climatic zones.
- The proposed method is based on employing automatic digital control circuits and integrating them into the SAH system combined with a wire mesh absorber technique for online temperature regulation to improve the heat transfer process represented by capturing and converting solar radiation quickly and easily into heat energy for various thermal applications and under different climate conditions.
- The study shows that, in comparison to maintaining a constant fan speed during daylight hours, altering the fan speed automatically to provide the appropriate air mass flow rate by temperature values provides energy savings and achieves temperature values that are balanced according to the required range. The automatic control for the solar air heater results in enhancing thermal efficiency by about 39.5%

Acknowledgements

The authors would like to thank the Energy and Renewable Energies Branch / Department of Electromechanical Engineering/ University of Technology for the technical support in conducting this work.

Nomenclature

A_c	Area of collector (m^2)
A_h	Duct cross-section area (m^2)
C_p	Air-specific heat (kJ/kg.K)
D_h	Equivalent hydraulic diameter (m)
I	Global solar radiation (W/m^2)
L	Hight of duct (m)
$\dot{m}_a$	Air mass flow rate (kg/s)
Q_u	Useful thermal gain (W)
R_e	Reynolds number
SAH	Solar air heater
t	Local time (hr)
T_i	Ambient temperature (°C)
T_{mesh}	Temperature of wire mesh of SAH (°C)
T_P	Temperature of flat plate of SAH (°C)
To_1	Temperature of outlet air of flat plate of SAH (°C)
To_2	Temperature of outlet air of wire mesh of SAH (°C)
v	Kinematic Viscosity (m^2/s)
V	Average velocity of air (m/s)
W	Width of duct (m)
η_{th}	Thermal efficiency of the heater (%)
ρ	Air Density (kg/m^3)
ΔT	Temperature difference (°C)

References

1) Y.-D. Kim, K. Thu, K.C. Ng, Evaluation and parametric optimization of the thermal performance and cost effectiveness of active-indirect solar hot water plants, *Evergreen,* 2(2) 50-60 (2015). https://doi.org/10.5109/1544080.
2) K. Tewari, R. Dev, Analysis of modified solar water heating system made of transparent tubes & insulated metal absorber. Evergreen, 5(1) 62-72 (2018). https://doi.org/10.5109/1929731.
3) S. Karsli, Performance analysis of new-design solar air collectors for drying applications, Renewable Energy 32 (10) (2007) 1645-1660. https://doi.org/10.1016/j.renene.2006.08.005.
4) A.Pramod, A. Kumar, A. Dubey, I. Mani, Development of microcontroller-based data logger for real-time monitoring of drying and storage of food grains, *Agricultural Engineering Today*, 45 (1) 2021. https://doi.org/10.52151/aet2021451.1528.
5) L. A Alkahdery, A.V. Yurchenko, J.A.-K. Mohammed, A.D. Mekhtiyev, Y.G. Neshina, PERFORMANCE IMPROVEMENT OF SOLAR DRYER USING AN AUXILIARY HEAT SOURCE UNDER DIFFERENT VALUES OF AIRFLOW RATES,

Eurasian Physical Technical Journal, 20, 1(43) (2023) 42-50. https://doi.org/10.31489/2023No1/42-50.

6) G.O. Pasetti, J.E. Normey-Rico, Automation and energy optimization of a domestic solar heating unit, *2014 5th International Renewable Energy Congress (IREC)*, https://doi.org/10.1109/IREC.2014.6826926.
7) KP.K. Choudhury, D.C. Baruah, "Solar air heater for residential space heating". Energy, *Ecology and Environment* 2 (6) (2017) 387–403. https://doi.org/10.1007/s40974-017-0077-4.
8) F. Ozgen, M. Esen, H. Esen, Experimental investigation of thermal performance of a double-flow solar air heater having aluminum cans, *Renewable Energy* 34 (11)(2009) 2391-2398. https://doi. org/ 10.1016/j.renene.2009.03.029.
9) M. H. Benli, Experimentally derived efficiency and exergy analysis of a new solar air heater having different surface shapes, *Renewable Energy* 50 (2013)58-67.https://doi.org/10.1016/j.renene.2012. 06.022.
10) Jessam, Raed A., Hussain H. Al-Kayiem, and Mohammed S. Nasif. "Flow control in s-shaped air intake diffuser of gas turbine using proposed energy promoters." In *MATEC web of conferences*, vol. 131, p. 02006. EDP Sciences, 2017.
11) Jessam, Raed A., Hussain H. Al-Kayiem, and Mohammed Shakir Nasif. "CFD simulation of flow control with energy promoters in S-shaped diffuser." (2017).
12) Jessam, Raed A., Hussain H. Al-Kayiem, and Mohammad S. Nasif. "Flow control in s-shaped aggressive diffuser using grooves on the inner and outer surfaces." (2016).
13) K. Kulkarni, K.-Y. Kim, Comparative study of solar air heater performance with various shapes and configurations of obstacles, Heat and Mass Transfer, 52 (2016) 2795-2811. https://doi.org/10.1007/s00231-016-1788-3.
14) J.M. Jalil, K.F. Sultan, L.A. Rasheed, Numerical and Experimental Investigation of Solar Air Collectors Performance Connected in Series, *Eng. & Tech. Journal* 35 (3) (2017) 190-196. https://doi.org/10.30684/etj.35.3A.2.
15) S. Singh, L. Dhruw, S. Chander, Experimental investigation of a double pass converging finned wire mesh packed bed solar air heater, *Journal of Energy Storage* 21 (2019) 713–723. https://doi.org/10.1016/j.est.2019.01.003.
16) J. M. Jalil, R.F. Nothim, M.M. Hameed, Effect of Wavy Fins on Thermal Performance of Double Pass Solar Air Heater, *Eng. & Tech. Journal*, 39 (9) (2021) 1362-1368. https://doi.org/10.30684/etj.v39i9.1775 .
17) A.A. Ismaeel, H.A.A. Wahhab, and Z.H. Naji, Performance evaluation of updraft air tower power plant integrated with double skin solar air heater, *Evergreen,* 8(2) 296–303 (2021). https://doi.org/10.5109/4480706.
18) R. Kumar, S.K. Verma, N.K. Gupta, S.K. Singh, Performance Enhancement of TSAH using Graphene and Graphene/CeO2 -Black Paint Coating on Absorber: A Comparative Study, *Evergreen* 9(3) 673-681 (2022). https://doi.org/10.5109/4843098.
19) N.F. Hussein, S.T. Ahmed, A.L. Ekaid, Thermal Performance of a Counter-Flow Double-Pass Solar Air Heater With The Steady and Pulsating Flow, Eng. & Tech. Journal, 41 (1) (2023) 176-184. https://doi.org/10.30684/etj.2022.135475.1274.
20) L.A. Rasheed, J.A.-K. Mohammed, Jessam, Raed A., Performance Enhancement of a Single Pass Solar Air Heater by Adopting Wire Mesh Absorber Layer, *Evergreen,* 10(2) 880-887 (2023). https://doi.org/10.5109/6792883
21) V. Bhatia, G. Bhatia, Room Temperature based Fan Speed Control System using Pulse Width Modulation Technique, *International Journal of Computer Applications* 81 (5)(2013) 35–40. https://doi.org /10.5120/14011-2067.
22) K. Kesarwani, S.M. Pranav, T.N. Noah, K.V.N. Kavitha, Design of Temperature Based Speed Control System Using Arduino Microcontroller, *Int. J. Chem. Sci.* 14 (S3) (2016) 753–760.
23) W. Widhiada, D.N.K.P. Negara, P.A. Suryawanm, Temperature Distribution Control for Baby Incubator System Using Arduino ATMega 2560. *Bali Indonesia* 19 (10) part XV (2017) 1748–1751.
24) R. Abdullah, Z.I. Rizman, N.N.S.N. Dzulkefli, S. Ismail, R. Shafie, M.H. Jusoh, Design an Automatic Temperature Control System for Smart Tudung Saji Using Arduino Microcontroller, *ARPN Journal of Engineering and Applied Sciences* 11 (16) (2016) 9578–9581.
25) L. Yu, Q. Zhang, X. Meng, Z. Yan, Design of the granary temperature and humidity measure and control system based on Zigbee wireless sensor network. *2011 IEEE International Conference on Electrical and Control Engineering*. https://doi.org/10.1109/ICECENG.2011.6057835.
26) S. Badhiye, D. Chatur, P. Wakode, Data logger system: A Survey, *In the proceedings of the National Conference on Emerging Trends in Computer Science and Information Technology (NCETSIT)* held on March 11, 2011 at Mumbai, pp. 24-26.
27) D. Fisher, P. Gould, Open-source hardware is a low-cost alternative for scientific instrumentation and research. *Modern instrumentation* 1 (2) (2012) 8-20. https://doi.org/10.4236/mi.2012.12002.
28) J. Rajmond, D. Pitică, Data logger for signal analysis and failure prediction, *2010 IEEE 16th International Symposium for Design and Technology in Electronic Packaging (SIITME)*. https://doi.org/10.1109/SIITME.2010.5650787.
29) A. Suzdalenko, A. Lazdans, I. Galkin, Development of multi-channel analogue signal data logger based on

MSP430, *2012 5th European DSP Education & Research Conference (EDERC)*. https://doi.org/10.1109/EDERC.2012.6532221.

30) Y. Lan, X. Lin, M.F. Kocher, W.C. Hoffmann, Development of a PC-based Data Acquisition and Control System, *Agricultural Engineering International: CIGR Journal*, 6 (5) (2007) 1-11.
31) M. Pradhapraj, H. Sivarathinamoorthy, Development of Monitoring System for the Solar Air Heater, *International Journal of Printing, Packaging & Allied Sciences* 5 (1)(2017) 167-176
32) S.A. Jumaat, M.H. Othman, Solar Energy Measurement Using Arduino*, MATEC Web of Conferences* 150 (01007) (2018). https://doi.org/10.1051/matecconf/201815001007.
33) Jessam, Raed A., and Han J. Chua. "Experimental Evaluation of a Hybrid Inclined Solar Chimney for Power Generation." *International Journal of Energy Production and Management. 2023. Vol. 8. Iss. 2* 8, no. 2 (2023): 81-87. https://doi.org/ 10.18280/ijepm.080204